

PROMPT OPTIMIZATION ACROSS MULTIPLE AGENTS FOR REPRESENTING DIVERSE HUMAN POPULATIONS

Manh Hung Nguyen
 MPI-SWS, Germany
 manguyen@mpi-sws.org

Sebastian Tschiatschek
 University of Vienna, Austria
 sebastian.tschiatschek@univie.ac.at

Adish Singla
 MPI-SWS, Germany
 adishs@mpi-sws.org

ABSTRACT

The difficulty and expense of obtaining large-scale human responses make Large Language Models (LLMs) an attractive alternative and a promising proxy for human behavior. However, prior work shows that LLMs often produce homogeneous outputs that fail to capture the rich diversity of human perspectives and behaviors. Thus, rather than trying to capture this diversity with a single LLM agent, we propose a novel framework to construct a set of agents that collectively capture the diversity of a given human population. Each agent is an LLM whose behavior is steered by conditioning on a small set of human demonstrations (task–response pairs) through in-context learning. The central challenge is therefore to select a representative set of LLM agents from the exponentially large space of possible agents. We tackle this selection problem from the lens of submodular optimization. In particular, we develop methods that offer different trade-offs regarding time complexity and performance guarantees. Extensive experiments in crowdsourcing and educational domains demonstrate that our approach constructs agents that more effectively represent human populations compared to baselines. Moreover, behavioral analyses on new tasks show that these agents reproduce the behavior patterns and perspectives of the students and annotators they are designed to represent.

1 INTRODUCTION

The growing deployment of Large Language Models (LLMs) as human proxies in research and industry has revealed a critical limitation: these models often produce homogeneous outputs that fail to capture the rich diversity of human perspectives and behaviors (Bao et al., 2024; Wenger & Kenett, 2025; Lee et al., 2024; Lahoti et al., 2023). This issue limits their applicability in domains that require this rich diversity, e.g., NLP tasks such as text paraphrasing (Cegin et al., 2023), simulating human behaviors and opinions in surveys (Xie et al., 2024; Santurkar et al., 2023), evaluating conversational recommendation systems (Yoon et al., 2024), replicating human subject studies (Aher et al., 2023), and simulating diverse roles in educational contexts (Nguyen et al., 2024; Markel et al., 2023; Zhang et al., 2025). In particular, LLMs might not be suitable for statistical inference and pose risks of reinforcing and potentially amplifying prevailing community norms in such domains.

To address these limitations, existing works have explored various approaches to align LLMs with humans. A common approach is to fine-tune a single LLM to align with human preferences, e.g., via Reinforcement Learning from Human Feedback (RLHF) (Ouyang et al., 2022). However, RLHF typically relies on aggregated preferences, which can obscure minority viewpoints and may be unrepresentative of broader populations (Casper et al., 2023; Kirk et al., 2023). Indeed, research suggests that it is fundamentally challenging, if not infeasible, to train one model to simultaneously satisfy a multitude of diverse, potentially conflicting, preferences (Ouyang et al., 2022). Another line of work focuses on test-time alignment, which avoids re-training or fine-tuning and leverages in-context learning capabilities of generative models (Brown et al., 2020). In particular, these approaches adapt model behavior dynamically by “conditioning” LLMs on personas or demographic attributes from humans, using techniques such as in-context impersonation (Salewski et al., 2023), culturally specific prompting (Tao et al., 2024), and demographic-aware prompting (Aher et al., 2023).

In this work, we shift the focus from creating a single agent that represents a human population to constructing a set of representative agents. Figure 1 provides an overview of our approach. Our

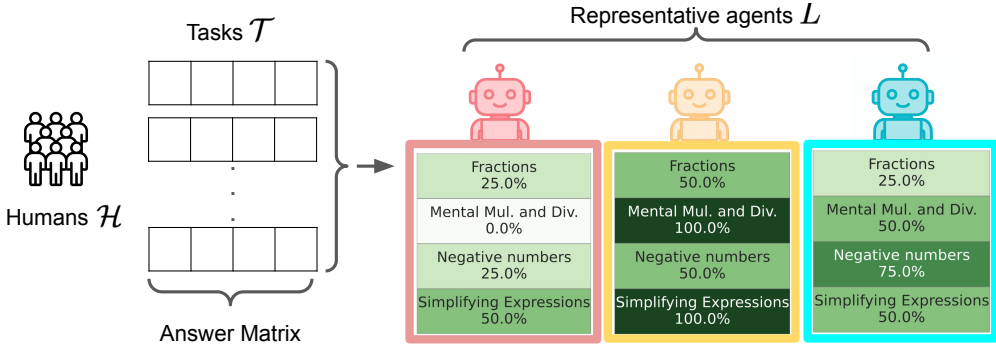


Figure 1: Illustrative example of constructing a set of agents L that is representative of a given human population \mathcal{H} . In this example, \mathcal{H} is a group of diverse students working on a set of tasks \mathcal{T} and providing answers. The goal is to create a set of agents L that can accurately represent the students. The resulting agents exhibit different levels of understanding across mathematical concepts, with each agent corresponding to a group of students matched by skill level and task performance.

guiding hypothesis is that a carefully curated ensemble of diverse agents can collectively achieve a more faithful representation of a given human population. We approach this by leveraging the power of in-context learning, where an agent’s behavior is steered by a small set of behavior-representative demonstration examples provided in its prompt. To this end, we formulate the problem of constructing an optimal set of agents as a joint optimization of their prompts. To make this problem tractable, we cast it as a submodular optimization problem and propose several methods for solving it, offering different trade-offs regarding time complexity and performance. Our experimental evaluation shows that these methods can construct agents representative of different groups of people, and that the agents exhibit behaviors matching those groups on new tasks. In summary, our main contributions are:

- We propose a novel formulation that casts the construction of a representative set of LLM agents for a diverse human population as a submodular optimization problem (§3).
- We instantiate this submodular optimization framework and propose methods for selecting sets of representative agents, offering trade-offs between computational tractability and performance (§4).
- We empirically demonstrate the efficiency of our approach in constructing agents that capture the behavior of a given human population in educational and crowdsourcing settings (§5).
- We conduct behavioral analysis on new tasks and show that agents constructed by our methods exhibit behaviors similar to the students and annotators they are intended to represent (§5).

2 RELATED WORK

LLMs for crowdsourcing and simulating human behaviors. Large language models have emerged as tools for facilitating crowdsourcing tasks and simulating human behaviors. The applications of these models have expanded across multiple domains, enabling research at speed and scale while reducing potential risks to human crowdworkers. Recent studies have demonstrated LLMs’ effectiveness as virtual crowd workers for various Natural Language Processing tasks, including data annotation (Moskovskiy et al., 2024), text paraphrasing (Cegin et al., 2023), named entity recognition and relation extraction (Zhang et al., 2023), and text classification (Sun et al., 2023). Another line of work investigated LLMs’ capacity for simulating human behaviors and opinions (Xie et al., 2024; Santurkar et al., 2023), evaluating conversational recommendation systems (Yoon et al., 2024), replicating human subject studies (Aher et al., 2023), and simulating diverse roles in educational contexts (Nguyen et al., 2024; Markel et al., 2023; Zhang et al., 2025).

Diversity and biases and in LLMs outputs. Current LLMs produce outputs with low diversity and biases, making them unrepresentative of many population groups. Studies have revealed systematic homogeneity in LLM responses (Yoon et al., 2024) and significant divergence from the distribution of real human survey responses (Sun et al., 2024). These limitations may stem from sociocultural biases observed since early models (Brown et al., 2020), creating substantial misalignment with numerous

demographic groups (Santurkar et al., 2023; Tao et al., 2024). The "hyper-accuracy distortion" in human subject study replication (Aher et al., 2023) further demonstrates LLMs' failure to capture diverse viewpoints. Together, these findings highlight fundamental limitations in representing population diversity, raising concerns about LLMs' reliability for statistical inference and their tendency to encode and perpetuate dominant community norms (Bender et al., 2021; Liu et al., 2024). Our work aims at making outputs from LLMs more diverse and representative of a given human population.

Inducing and aligning behaviors of LLMs. Recent work has explored techniques to mitigate diversity and representational issues by aligning LLMs with different population groups. LLMs are often treated as a superposition of perspectives (Kovac et al., 2023), which allows different prompting strategies without modifying model parameters, such as in-context impersonation (Salewski et al., 2023) and demographic-aware prompting (Santurkar et al., 2023). Another line of work involves training or fine-tuning models for cross-cultural alignment (Ramezani & Xu, 2023), value alignment (Liu et al., 2022). Our work builds upon the success of leveraging in-context learning and prompting techniques, but differs in a sense that we focus on optimizing prompts for multiple agents to collectively represent a diverse human population, without using demographic information or metadata.

3 PROBLEM FORMULATION

In this section, we first introduce the necessary notation and background. We then formally define the problem of selecting a representative set of agents and our optimization objective.

3.1 PRELIMINARIES

Let $\mathcal{H} = \{h_1, h_2, \dots, h_N\}$ denote a population of N humans we want to represent. We assume access to demonstrations (e.g., task-response pairs) from \mathcal{H} on a set of tasks \mathcal{T} , denoted by $\mathcal{D}_{\mathcal{H}}^{\mathcal{T}}$. If each human provides a response to every task, then $|\mathcal{D}_{\mathcal{H}}^{\mathcal{T}}| = |\mathcal{H}| \times |\mathcal{T}|$. Each human h is represented by a vector $\mathbf{e}_h \in \mathbb{R}^d$ that summarizes their behavior across the tasks in \mathcal{T} . We define an agent l as an LLM conditioned on a set of K demonstrations, where each demonstration is a task-response pair. The demonstrations are used to steer the agent's behavior through in-context learning. The space of all possible agents that can be constructed from $\mathcal{D}_{\mathcal{H}}^{\mathcal{T}}$ is denoted by $|\mathcal{L}| = \binom{|\mathcal{D}_{\mathcal{H}}^{\mathcal{T}}|}{K}$. This number is finite but typically much larger than $|\mathcal{H}|$. When K is fixed, $|\mathcal{L}|$ asymptotically scales as $(|\mathcal{T}| \cdot |\mathcal{H}|)^K$, which we use later for complexity analysis. Similar to humans, each agent l is represented by a vector $\mathbf{e}_l \in \mathbb{R}^d$ that captures its behavior across tasks in \mathcal{T} . In our experiments (Section 5), we explore several types of behavioral embeddings, including binary vectors of student performance, vectors of individuals' answer choices, and continuous semantic embeddings of annotators' responses.

We measure the behavioral similarity between any two objects (humans or agents) by the distance between their embedding vectors, defined as $dist(\mathbf{e}_1, \mathbf{e}_2)$ (e.g., Euclidean distance). The *representation gap* of a set of agents $L \subseteq \mathcal{L}$ with respect to the population \mathcal{H} is the average distance between each human h and its closest agent $l \in L$, given by $g(L) = \frac{1}{|\mathcal{H}|} \sum_{h \in \mathcal{H}} \min_{l \in L} dist(\mathbf{e}_h, \mathbf{e}_l)$. This representation gap serves as a proxy for how well the selected agents capture the diverse behaviors and perspectives of the given population. As we will show in our experiments (Section 5), minimizing this gap leads to agents whose behaviors align closely with those of humans on unseen tasks.

3.2 OBJECTIVE

Our goal is to select a set of agents $L^{\text{opt}} \subseteq \mathcal{L}$ of size M that best represents the human population by minimizing the average distance between each human and its closest agent: $L^{\text{opt}} = \arg \min_{L \subseteq \mathcal{L}, |L| \leq M} g(L)$. We define the baseline gap when no agents are selected ($L = \emptyset$) as $g(\emptyset) = \frac{1}{|\mathcal{H}|} \sum_{h \in \mathcal{H}} D_{\text{max}}$, where D_{max} is a constant larger than any possible human-agent embedding distance. It is often more natural to view the problem as maximizing the gain relative to this baseline. We therefore define the average distance reduction obtained by selecting a set L as:

$$f(L) = g(\emptyset) - g(L) = \frac{1}{|\mathcal{H}|} \sum_{h \in \mathcal{H}} \left[D_{\text{max}} - \min_{l \in L} dist(\mathbf{e}_h, \mathbf{e}_l) \right] \quad (1)$$

Table 1: Performance guarantees and time complexity analysis.

| Method | Performance Guarantee | Time Complexity |
|-----------------------------------|---|---|
| OPT | $f(L^{\text{opt}})$ | $\mathcal{O}((\mathcal{T} \cdot \mathcal{H})^{KM})$ |
| SINGLE | — | $\mathcal{O}(1)$ |
| RANDOM | — | $\mathcal{O}(M)$ |
| GREEDY | $(1 - \frac{1}{e}) \cdot f(L^{\text{opt}})$ | $\mathcal{O}(M \cdot \mathcal{H} \cdot (\mathcal{T} \cdot \mathcal{H})^K)$ |
| SAMPLEGREEDY | — | $\mathcal{O}(M \cdot \mathcal{H} \cdot \psi \cdot (\mathcal{T} \cdot \mathcal{H})^K)$ |
| REPPOP _{demo} (ours) | — | $\mathcal{O}(M \cdot K \cdot \mathcal{T} \cdot \mathcal{H} ^2)$ |
| REPPOP _{mapped-1} (ours) | $(1 - 1/e) \cdot (\gamma \cdot f(L^{\text{opt}}) - \rho)$ | $\mathcal{O}(K \cdot \mathcal{H} + M \cdot \mathcal{H} ^2)$ |
| REPPOP _{mapped-2} (ours) | $(1 - 1/e) \cdot (\gamma \cdot f(L^{\text{opt}}) - \rho)$ | $\mathcal{O}(K \cdot \mathcal{T} \cdot \mathcal{H} + M \cdot \mathcal{H} ^2)$ |

This gives us a monotone submodular function $f(L)$ that can be approximated using greedy algorithms. The optimization problem is therefore to find $L^{\text{opt}} = \arg \max_{L \subseteq \mathcal{L}, |L| \leq M} f(L)$.

4 METHODOLOGY

In this section, we establish the hardness of the representative agent selection problem and prove the submodularity of our objective function. We then discuss how naive applications of existing strategies are insufficient and present improved methods in Section 4.2. The performance guarantees and time complexity of the methods discussed in this section are summarized in Table 1.

4.1 HARDNESS OF THE PROBLEM AND CONNECTION TO SUBMODULARITY

Theorem 1 (NP-Hardness). *The problem of selecting an optimal subset $L^* \subseteq \mathcal{L}$ of size M that maximizes $f(L)$ is NP-hard.*

Proof sketch. We show NP-hardness through a reduction from the uncapacitated facility location problem (UFLP) with zero facility costs, which is known to be NP-hard (Verter, 2011). We provide a detailed proof of this proposition in Appendix D.1.

Proposition 1 (Submodularity of the Objective Function $f(L)$). *The objective function $f(L) = \frac{1}{|\mathcal{H}|} \sum_{h \in \mathcal{H}} [D_{\max} - \min_{l \in L} \text{dist}(\mathbf{e}_h, \mathbf{e}_l)]$ is submodular.*

Proof sketch. Our objective function $f(L)$ exhibits the diminishing returns property of submodularity, which follows directly from its connection to the facility location problem (Krause & Golovin, 2014). We provide proof of this proposition in Appendix D.2.

Greedy Approximation. Due to the NP-hardness of the problem, finding the optimal solution L^{opt} requires exhaustive search with time complexity $\mathcal{O}((|\mathcal{T}| \cdot |\mathcal{H}|)^{KM})$. The submodularity of our objective function enables the GREEDY algorithm to achieve a $(1 - 1/e) \cdot f(L^{\text{opt}})$ -approximation guarantee (Nemhauser et al., 1978), with time complexity $\mathcal{O}(M \cdot |\mathcal{H}| \cdot (|\mathcal{T}| \cdot |\mathcal{H}|)^K)$. However, this approach becomes intractable as the agent space grows. A stochastic variant, STOCHASTICGREEDY, samples a subset of agents at each iteration to approximate the solution (Mirzasoleiman et al., 2015), but this still remains impractical for large spaces. Inspired by (Singla et al., 2014; Mirzasoleiman et al., 2015), we adopt SAMPLEGREEDY, which fixes a candidate pool \mathcal{C} containing only a fraction ψ of agents from \mathcal{L} and applies greedy selection within this pool. At each round, the marginal contribution of each remaining agent in \mathcal{C} is evaluated relative to the current set, and the best agent is added. This process continues until M agents are selected. The time complexity is $\mathcal{O}(M \cdot |\mathcal{H}| \cdot \psi \cdot (|\mathcal{T}| \cdot |\mathcal{H}|)^K)$, which is still impractical for large populations and motivates the more efficient methods introduced in the next section.

4.2 OUR PROPOSED METHODS

Greedy selection of demonstrations for an agent’s context. Searching through the exponentially large agent space \mathcal{L} is computationally infeasible, limiting the practicality of standard greedy methods. Hence, we propose an alternative method, REPPOP_{demo} (**R**epresentative **P**opulation using **d**emonstration-level greedy selection), which reduces the complexity to $\mathcal{O}(M \cdot K \cdot |\mathcal{T}| \cdot |\mathcal{H}|^2)$ and

Algorithm 1 Greedy selection of demonstrations (REPPOP_{demo})

- 1: **Input:** Human set \mathcal{H} , human demonstrations $\mathcal{D}_{\mathcal{H}}^{\mathcal{T}}$, number of agents to select M , context size K
- 2: **Output:** A set of representative agents $L \subseteq \mathcal{L}$ with $|L| \leq M$
- 3: Initialize $L \leftarrow \emptyset$
- 4: **for** $i = 1$ to M **do**
- 5: Initialize $\Omega \leftarrow \emptyset$ ▷ Best set of K demonstrations found so far
- 6: **for** $k = 1$ to K **do**
- 7: $demo^* \leftarrow \arg \max_{demo \in \mathcal{D}_{\mathcal{H}}^{\mathcal{T}} \setminus \Omega} f(L \cup \{l_{\Omega \cup \{demo\}}\}) - f(L)$ ▷ Select demo.
- 8: $\Omega \leftarrow \Omega \cup \{demo^*\}$
- 9: $L \leftarrow L \cup \{l_{\Omega}\}$ ▷ Add agent with context Ω to solution set
- 10: **return** L

Algorithm 2 Greedy selection of human-mapped agents (REPPOP_{mapped-1} and REPPOP_{mapped-2})

- 1: **Input:** Human set \mathcal{H} , human demonstrations $\mathcal{D}_{\mathcal{H}}^{\mathcal{T}}$, number of agents to select M , context size K
- 2: **Output:** A set of representative agents $L \subseteq \mathcal{L}$ with $|L| \leq M$
- 3: Initialize $\tilde{\mathcal{L}} \leftarrow \emptyset, L \leftarrow \emptyset$
- 4: **for** each human $h \in \mathcal{H}$ **do**
- 5: Create agent l_h using a subset of K demonstrations from $\mathcal{D}_h^{\mathcal{T}}$ ▷ Human-mapped agent
- 6: $\tilde{\mathcal{L}} \leftarrow \tilde{\mathcal{L}} \cup \{l_h\}$ ▷ Add the agent to pool
- 7: **for** $i = 1$ to M **do**
- 8: $l^* \leftarrow \arg \max_{l \in \tilde{\mathcal{L}} \setminus L} f(L \cup \{l\}) - f(L)$ ▷ Select agent
- 9: $L \leftarrow L \cup \{l^*\}$ ▷ Add agent to solution set
- 10: **return** L

empirically achieves competitive performance. Instead of enumerating all candidate agents and evaluating their marginal gains, REPPOP_{demo} builds each agent incrementally (cf. Algorithm 1). At each step it greedily selects a demonstration from the pool $\mathcal{D}_{\mathcal{H}}^{\mathcal{T}}$ to extend the current context Ω . We denote by l_{Ω} the agent constructed from Ω . This demonstration-level greedy construction avoids the exponential blow-up in $|\mathcal{L}|$, but sacrifices the formal performance guarantee of standard greedy selection.

Greedy selection of human-mapped agents. To further address the computational intractability of searching the full agent space \mathcal{L} , we introduce a reduced pool of proxies that directly reflect the humans in the population. We construct $\tilde{\mathcal{L}} = \{l_h \mid h \in \mathcal{H}\}$, where each agent l_h corresponds to a human $h \in \mathcal{H}$ and is formed by conditioning on a subset of K demonstrations from $\mathcal{D}_h^{\mathcal{T}}$. This one-to-one mapping reduces the candidate space to $|\tilde{\mathcal{L}}| = |\mathcal{H}|$ while preserving diversity. The selection problem then becomes $L^* = \arg \max_{L \subseteq \tilde{\mathcal{L}}, |L| \leq M} f(L)$. Building on this human-centered mapping idea, we instantiate two methods, REPPOP_{mapped-1} and REPPOP_{mapped-2}, which both follow the general procedure in Algorithm 2. Their only difference lies in how demonstrations are selected to construct a human-mapped agent (line 5). In REPPOP_{mapped-1}, the K demonstrations for each human are sampled uniformly at random, yielding lightweight proxy agents with cost $\mathcal{O}(K|\mathcal{H}|)$. In contrast, REPPOP_{mapped-2} selects the K demonstrations greedily with respect to the human's own behavior, producing stronger proxies at cost $\mathcal{O}(K|\mathcal{T}||\mathcal{H}|)$. Concretely, for each human h , the demonstrations are chosen to minimize the distance between the human's embedding e_h and the embedding of the constructed agent e_{l_h} , i.e., $\text{dist}(e_h, e_{l_h})$. Both methods share the same greedy selection stage over the proxy pool, which requires $\mathcal{O}(M|\mathcal{H}|^2)$ time, and both enjoy the same approximation guarantee in Theorem 2.

Theorem 2 (Performance Guarantee for REPPOP_{mapped-1} and REPPOP_{mapped-2}). *Let $\tilde{\mathcal{L}} = \{l_h \mid h \in \mathcal{H}\}$ be the proxy agent set where for each $h \in \mathcal{H}$, $l_h \in N_{\rho}(h)$, with $N_{\rho}(h)$ representing the ρ -neighborhood of h . Define the human coverage ratio $\gamma = f(L_{\mathcal{H}}^*)/f(L_{\mathcal{L}}^*) \in [0, 1]$, where $L_{\mathcal{H}}^*$ is the optimal subset from the human set and $L_{\mathcal{L}}^*$ is the optimal subset from the full agent set. If $L_{\tilde{\mathcal{L}}}^{\text{greedy}}$ is the subset of size M returned by the greedy algorithm on $\tilde{\mathcal{L}}$, then:*

$$f(L_{\tilde{\mathcal{L}}}^{\text{greedy}}) \geq (1 - 1/e) (\gamma \cdot f(L_{\mathcal{L}}^*) - \rho),$$

where γ measures the cost of restricting the search space to humans (coverage quality) and ρ measures the cost of approximating each human by a proxy agent (imitation error). The value of γ is determined by how expressive the human set is relative to the full agent space, whereas ρ depends on the proxy construction strategy: uniform sampling in REPPOP_{mapped-1} typically yields larger ρ , while greedy selection in REPPOP_{mapped-2} achieves smaller ρ at the expense of higher computational cost.

Table 2: Statistics of datasets used in our experiments.

| Dataset | Domain | Task Type | Repr. Type | Multimodal | No. Humans | No. Tasks | Source |
|-----------|------------------|--------------|-------------|------------|------------|-----------|--------------------------------|
| EEDI | Education | Multi-choice | Performance | No | 50 | 40 | Primary & High school students |
| OpinionQA | Opinion Survey | Multi-choice | Opinion | No | 500 | 77 | US citizen |
| Wikiart | Image Annotation | Open-ended | Semantic | Yes | 100 | 20 | LLM-based annotators |

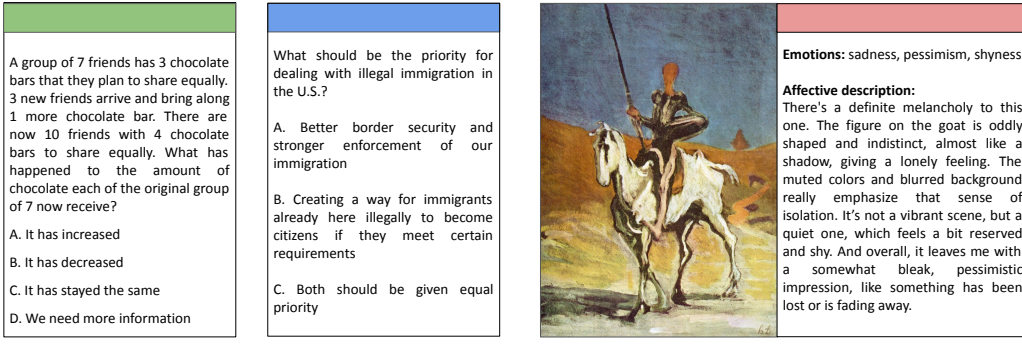


Figure 2: Examples of tasks in our experiments.

Proof sketch. We show that for the optimal human subset $L_{\mathcal{H}}^*$, the corresponding set of proxy agents $L_{\tilde{\mathcal{H}}}^* = \{l_h | h \in L_{\mathcal{H}}^*\} \subseteq \tilde{\mathcal{L}}$ satisfies $f(L_{\tilde{\mathcal{H}}}^*) \geq f(L_{\mathcal{H}}^*) - \rho$ due to the ρ -neighborhood property. Since $L_{\tilde{\mathcal{L}}}^*$ is optimal within $\tilde{\mathcal{L}}$, we have $f(L_{\tilde{\mathcal{L}}}^*) \geq f(L_{\mathcal{H}}^*)$. By the standard greedy approximation for submodular functions, $f(L_{\tilde{\mathcal{L}}}^{\text{greedy}}) \geq (1 - 1/e)f(L_{\tilde{\mathcal{L}}}^*)$. Combining these inequalities and using the human coverage ratio $\gamma = f(L_{\mathcal{H}}^*)/f(L_{\mathcal{L}}^*)$, we derive our bound. We provide complete proof in Appendix D.3.

5 EXPERIMENTAL EVALUATION

In this section, we present the evaluation domains and datasets (see Table 2 for summary statistics), describe the methods evaluated, and discuss the main results, with additional setup details in Appendix B and further results in Appendix C.

5.1 EVALUATION DOMAINS AND DATASETS

Education: Math Questions and Answers (EEDI). In this domain, LLMs capturing the behavior of a diverse student population, can allow teachers to practice instructional strategies (Markel et al., 2023) and to conduct virtual pretesting (Benedetto et al., 2024) in a safe environment. Representing students with varying levels of skills and misconceptions can thus benefit both teachers and learners. To this end, we evaluate whether our methods can faithfully represent such a diverse group of students. Specifically, we use the EEDI dataset (Wang et al., 2020), which contains multiple-choice math questions and answers collected from students. Figure 2a shows an example question. We select 50 students and 40 exercises (tasks) from the dataset, splitting tasks and their corresponding answers 50/50 into the training and testing sets. Each student is represented by a binary embedding vector indicating their correct and incorrect answers to the math questions. The representation gap is measured using the L1 distance, which in this case is equivalent to the Hamming distance. Intuitively, it counts the number of questions on which two students' answers differ, reflecting their performance difference.

Crowdsourcing: Opinion Survey (OpinionQA). In this application, LLMs can be used as surrogates for crowdworkers, giving answers that reflect different opinions and beliefs that diverse groups of people might express. We use the OpinionQA dataset (Santurkar et al., 2023), which contains multiple-choice questions from the Pew American Trends Panel (ATP) surveys along with human responses. In particular, we focus on the ATP W92 survey, which includes 77 questions related to politics. Figure 2b shows an example question. From this dataset, we sample 500 people and their responses, and split the survey questions into 40 training and 37 test tasks. For each question, answer choices are mapped to ordinal values and normalized to the range $[-1, 1]$. Each human is represented

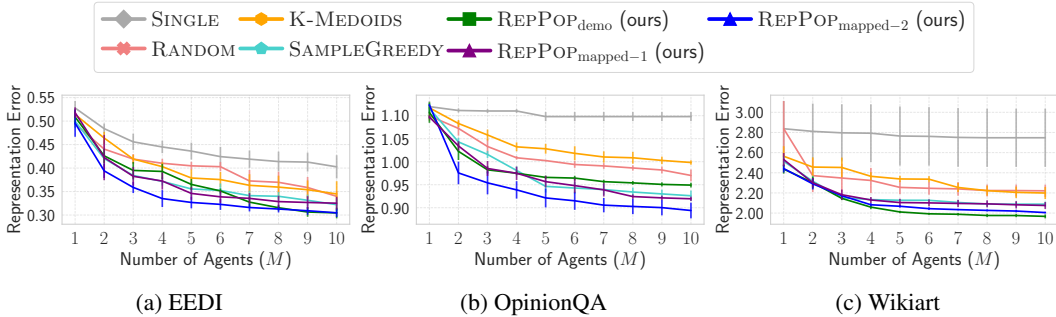


Figure 3: Representation error on test set. We show the representation error on the test set of each method with different number of agents. We report the means and standard errors (error bars) of three runs with different seeds. Our methods maintain lower representation error compared to baselines.

by a vector embedding of their responses, and the representation gap is measured using the L2 distance. This distance captures the extent of differences in opinions and beliefs expressed in their answers.

Crowdsourcing: Data Annotation (WikiArt). In this application, LLMs can be used as surrogates for crowdworkers for data annotation. We focus on tasks where diverse perspectives are encouraged. For example, to create a datasets on the emotions evoked by art (Mohammad & Kiritchenko, 2018; Mohamed et al., 2022), human crowdworkers were shown a painting and asked to specify the emotions it evoked and to provide a short affective description. Figure 2c shows an example of such a task. Our goal is to construct a set of LLM agents representative of a given pool of annotators in terms of both emotions and language use. We take 20 paintings from the WikiArt dataset (Tan et al., 2019) and split them 50/50 into training and testing tasks. Unfortunately, existing datasets do not provide annotations at the level of individual annotators, and thus we cannot use them directly in our experiments. Hence, we generated 100 “synthetic humans” by prompting LLMs with different “personalities” and asking them to annotate the paintings. Each annotator is then represented by a continuous embedding of their responses extracted from an LLM (cf. Appendix C.3 for details and alternative embedding strategies). Distances between these embeddings are computed using the L2 distance, which captures differences in annotators’ perspectives and behaviors across tasks.

5.2 METHODS EVALUATED

We compare our proposed methods $\text{REPPOP}_{\text{demo}}$, $\text{REPPOP}_{\text{mapped-1}}$, and $\text{REPPOP}_{\text{mapped-2}}$ from Section 4.2 against SAMPLEGREEDY from Section 4.1 and the following baselines. The SINGLE baseline uniformly samples a single agent from \mathcal{L} and performs M rollouts, while RANDOM baseline uniformly selects M agents from \mathcal{L} and performs one rollout for each. The K -MEDOIDS baseline applies K -medoids clustering to form M clusters of humans, and for each cluster uniformly samples K demonstrations from the humans in that cluster to construct an agent; this approach requires re-clustering whenever a new agent is added. For SAMPLEGREEDY , we set the sample size to the number of humans in all experiments. For $\text{REPPOP}_{\text{demo}}$, we accelerate evaluation with a stochastic greedy variant that samples a subset of α demonstration candidates from the pool $\mathcal{D}_{\mathcal{H}}^{\mathcal{T}}$, setting $\alpha = 100$ for WikiArt and EEDI, and $\alpha = 1000$ for OpinionQA (values chosen based on the scale of $\mathcal{D}_{\mathcal{H}}^{\mathcal{T}}$). All agents are implemented with decoding temperature fixed at 1.0 across all experiments.

5.3 RESULTS

Representation gap. We compare the considered methods by measuring the representation gap on the test tasks $\mathcal{T}_{\text{test}}$. The error is normalized according to the distance used in each dataset: by d for the EEDI dataset, and by \sqrt{d} for the OpinionQA and WikiArt datasets. Figure 3 shows the normalized test representation error of agent sets constructed by each method using Gemma3-12B as the underlying LLM, with varying numbers of agents (training plots are provided in Appendix C). Using a randomly sampled set of N agents (RANDOM) reduces the representation error compared to using a single agent with N rollouts (SINGLE), emphasizing the importance of the problem addressed in this work. The heuristic method K -MEDOIDS does not improve over the simple baseline

Table 3: Generalization to other models. Representation error on the EEDI dataset with $M = 10$ and $K = 3$ across model families of varying sizes (4B–70B). Results are reported on the test set, with bold numbers indicating the lowest error. Our proposed methods consistently outperform baselines, demonstrating lower representation error across all tested models and highlighting the robustness of our framework independent of the underlying model choice.

| Method | Model | | | | | |
|----------------------------|--------------------|----------------|-----------------|------------------|-----------------|--------------------|
| | Phi-4-mini (4B) | Phi-4 (14B) | Qwen-3 (14B) | Gemma-3 (27B) | Qwen-3 (32B) | Llama-3.1 (70B) |
| SINGLE | 0.39 | 0.39 | 0.42 | 0.35 | 0.37 | 0.46 |
| RANDOM | 0.39 | 0.36 | 0.36 | 0.35 | 0.35 | 0.46 |
| K-MEDOIDS | 0.41 | 0.36 | 0.38 | 0.36 | 0.37 | 0.38 |
| SAMPLEGREEDY | 0.38 | 0.36 | 0.34 | 0.34 | 0.34 | 0.37 |
| REPPOP _{demo} | 0.37 | 0.30 | 0.33 | 0.31 | 0.33 | 0.35 |
| REPPOP _{mapped-1} | 0.38 | 0.35 | 0.34 | 0.32 | 0.35 | 0.38 |
| REPPOP _{mapped-2} | 0.35 | 0.33 | 0.30 | 0.32 | 0.35 | 0.38 |

Table 4: Average runtime (in minutes) for selecting an agent, reported as mean \pm standard error over three seeds. We use agent set size $M = 10$, context size $K = 3$, and the Gemma3-12B model.

| Method | Dataset | | | | | | | | |
|----------------------------|---------------|----------------|----------------|----------------|-----------------|------------------|----------------|----------------|----------------|
| | EEDI | | | OpinionQA | | | Wikiart | | |
| | $K = 1$ | $K = 3$ | $K = 5$ | $K = 1$ | $K = 3$ | $K = 5$ | $K = 1$ | $K = 3$ | $K = 5$ |
| SINGLE | 0.3 ± 0.0 | 0.3 ± 0.0 | 0.3 ± 0.0 | 0.6 ± 0.0 | 0.4 ± 0.0 | 0.4 ± 0.0 | 2.0 ± 1.0 | 1.8 ± 0.9 | 1.6 ± 0.6 |
| RANDOM | 0.3 ± 0.0 | 0.3 ± 0.0 | 0.3 ± 0.0 | 0.3 ± 0.0 | 0.3 ± 0.0 | 0.3 ± 0.0 | 3.2 ± 1.8 | 1.8 ± 0.8 | 1.6 ± 0.6 |
| K-MEDOIDS | 0.9 ± 0.0 | 1.1 ± 0.0 | 1.3 ± 0.0 | 1.6 ± 0.0 | 1.7 ± 0.0 | 0.9 ± 0.0 | 2.5 ± 0.0 | 1.9 ± 0.0 | 2.3 ± 0.0 |
| SAMPLEGREEDY | 0.6 ± 0.0 | 0.7 ± 0.0 | 0.8 ± 0.0 | 2.7 ± 0.1 | 2.8 ± 0.0 | 3.2 ± 0.0 | 2.2 ± 0.0 | 1.8 ± 0.0 | 2.2 ± 0.0 |
| REPPOP _{demo} | 6.4 ± 0.1 | 21.3 ± 0.2 | 40.1 ± 0.4 | 38.3 ± 0.3 | 108.4 ± 0.9 | 179.0 ± 31.7 | 16.4 ± 0.1 | 43.6 ± 0.3 | 78.2 ± 0.2 |
| REPPOP _{mapped-1} | 0.6 ± 0.0 | 0.7 ± 0.0 | 0.8 ± 0.0 | 2.7 ± 0.1 | 2.9 ± 0.0 | 3.2 ± 0.1 | 2.2 ± 0.0 | 1.8 ± 0.0 | 2.2 ± 0.0 |
| REPPOP _{mapped-2} | 5.9 ± 0.0 | 17.8 ± 0.0 | 30.9 ± 0.1 | 71.7 ± 0.3 | 197.1 ± 0.3 | 350.1 ± 0.9 | 20.2 ± 0.2 | 43.0 ± 0.1 | 66.8 ± 0.5 |

RANDOM. By exploiting the submodularity of the problem, SAMPLEGREEDY applies a greedy selection procedure on a sampled subset of agents and achieves lower representation error than the aforementioned baselines. Finally, our methods further reduce representation error across all datasets. Notably, REPPOP_{mapped-2} outperforms the strongest baseline SAMPLEGREEDY significantly on all three datasets, with $p < 0.01$ according to a paired t-test where pairs are formed by matching runs that share the same random seed and the same number of agents. These results demonstrate that our methods can construct agent sets that represent human population behavior and generalize effectively.

Generalization to other LLMs. We conduct experiments with a variety of models to examine how method performance changes across model families and sizes. Due to resource constraints, this analysis is limited to the EEDI dataset with $M = 10$ and $K = 3$. Table 3 shows that the same trends hold across different LLMs in terms of reducing representation error. Our proposed methods consistently outperform the baselines, achieving lower representation error on the test set across all tested models. These results highlight the robustness of our framework regardless of the underlying LLM.

Trade-offs between performance and computation. We investigate the trade-off between performance and computational cost of different methods. Table 4 reports the average runtime for selecting an agent (details of computational resources are provided in Appendix B.4). Our method REPPOP_{mapped-1} runs as fast as SAMPLEGREEDY while achieving slightly better performance. Both REPPOP_{demo} and REPPOP_{mapped-1} are more computationally expensive but offer more representative agent sets. In practice, these trade-offs should be considered when selecting a suitable method.

5.4 AGENT BEHAVIOR ANALYSIS

Beyond measuring the representation gap via embedding distances, we investigate whether the agents exhibit behaviors similar to the humans they represent in the EEDI and OpinionQA datasets (cf. Appendix C.3 for analysis on WikiArt). First, we analyze, for each agent, the behavior of the humans it represents. Figure 4 shows 2D embeddings of humans and agents constructed by our method REPPOP_{mapped-2}, computed on the training set. We observe that REPPOP_{mapped-2} constructs agents that cover different regions of the human embedding space, corresponding to distinct groups of humans. Next, we analyze whether these agents behave like the groups of people they are intended to represent.

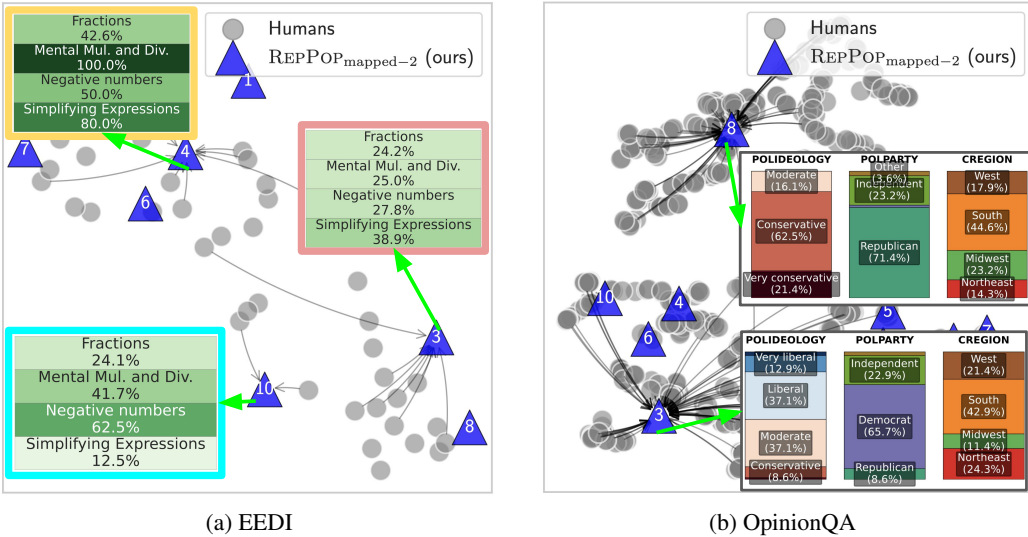


Figure 4: 2D embeddings of humans and agents constructed by $\text{REPOP}_{\text{mapped-2}}$ on tasks in $\mathcal{T}_{\text{train}}$ using UMAP. We provide examples of aggregated metadata (in the boxes) of humans represented by agents (connections are denoted by black arrows). They are not used for constructing agents and used only for analysis. Our method $\text{REPOP}_{\text{mapped-2}}$ constructs agents to cover different human behaviors, collectively (approximately) representing the human population. **(a) EEDI:** Each agent represents a group of students with particular success rates on different Math concepts. **(b) OpinionQA:** Each agent represents a group of people with particular distributions of political ideologies, parties, and regions.

EEDI dataset. We select three agents and visualize the students they represent, along with the aggregated math skill levels of those students in Figure 4a. For example, Agent 4 represents students with a strong understanding of Mental Multiplication and Division but weaker proficiency in Fractions and Negative Numbers. We then use these agents as surrogates for students to answer new math questions in the test data. The distinct proficiency levels of agents (3, 4, 10) on these new questions are shown in Figure 1, using the same color-coding of boxes. We find that their proficiency levels across different math concepts closely mirror those observed in the students they represent.

OpinionQA dataset. We select two agents and visualize the aggregated self-declared metadata of the humans they represent in Figure 4b. For each task in the test set, we map answer choices to political ideologies and party affiliations. For each agent, we compute the distribution over these labels across all questions. For example, for Agent 3 we obtain the following distributions: political ideologies — Very liberal (13.3%), Liberal (40%), Moderate (13.3%), Conservative (26.7%), Very conservative (6.2%); political parties — Independent (13.3%), Democrat (53.3%), Republican (33.3%). These distributions mirror the actual human demographic patterns for Agent 3 shown in Figure 4b, despite the fact that such metadata was not used in constructing the agents. These findings highlight their ability to capture and reproduce meaningful population-level diversity.

6 CONCLUDING DISCUSSIONS

We studied the problem of constructing a set of generative agents that collectively represent a given human population. Through formulating it as a submodular optimization problem, we proposed methods that allow different tradeoffs of computational complexity and performance (guarantees). In addition, we empirically demonstrated that our methods can construct a set of representative agents for different populations of annotators and students in crowdsourcing and educational settings. We also demonstrated quantitatively and qualitatively the generalizability of our methods to unseen tasks. Next, we would like to discuss the limitations of our work and propose directions for future research to tackle them. First, we rely on prompting-based approaches rather than fine-tuning; future work could explore fine-tuning techniques for constructing an agent. Second, we do not consider the ordering of demonstrations in prompts, and understanding how ordering influences model behavior would be a

valuable extension. Third, while our results show that agents constructed by our methods effectively represent a human population, this work primarily provides groundwork for more comprehensive evaluations of downstream applications, such as using the agents for training teachers, assessing the effectiveness of interventions, or simulating responses to government policy.

ACKNOWLEDGMENTS

Funded/Co-funded by the European Union (ERC, TOPS, 101039090). Views and opinions expressed are however those of the author(s) only and do not necessarily reflect those of the European Union or the European Research Council. Neither the European Union nor the granting authority can be held responsible for them.

REFERENCES

Gati V. Aher, Rosa I. Arriaga, and Adam Tauman Kalai. Using Large Language Models to Simulate Multiple Humans and Replicate Human Subject Studies. In *Proceedings of the International Conference on Machine Learning (ICML)*, 2023.

Keqin Bao, Jizhi Zhang, Yang Zhang, Xinyue Huo, Chong Chen, and Fuli Feng. Decoding Matters: Addressing Amplification Bias and Homogeneity Issue in Recommendations for Large Language Models. In *Proceedings of the 2024 Conference on Empirical Methods in Natural Language Processing (EMNLP)*, 2024.

Emily M. Bender, Timnit Gebru, Angelina McMillan-Major, and Shmargaret Shmitchell. On the Dangers of Stochastic Parrots: Can Language Models Be Too Big? In *ACM Conference on Fairness, Accountability, and Transparency (FAccT)*, 2021.

Luca Benedetto, Giovanni Aradelli, Antonia Donvito, Alberto Lucchetti, Andrea Cappelli, and Paula Buttery. Using LLMs to Simulate Students' Responses to Exam Questions. In *Findings of the Association for Computational Linguistics: EMNLP*, 2024.

Tom B. Brown, Benjamin Mann, Nick Ryder, Melanie Subbiah, Jared Kaplan, Prafulla Dhariwal, Arvind Neelakantan, Pranav Shyam, Girish Sastry, Amanda Askell, Sandhini Agarwal, Ariel Herbert-Voss, Gretchen Krueger, Tom Henighan, Rewon Child, Aditya Ramesh, Daniel M. Ziegler, Jeffrey Wu, Clemens Winter, Christopher Hesse, Mark Chen, Eric Sigler, Mateusz Litwin, Scott Gray, Benjamin Chess, Jack Clark, Christopher Berner, Sam McCandlish, Alec Radford, Ilya Sutskever, and Dario Amodei. Language Models are Few-Shot Learners. In *Advances in Neural Information Processing Systems 33: Annual Conference on Neural Information Processing Systems (NeurIPS)*, 2020.

Stephen Casper, Xander Davies, Claudia Shi, Thomas Krendl Gilbert, Jérémie Scheurer, Javier Rando, Rachel Freedman, Tomasz Korbak, David Lindner, Pedro Freire, Tony Tong Wang, Samuel Marks, Charbel-Raphaël Ségerie, Micah Carroll, Andi Peng, Phillip J. K. Christoffersen, Mehul Damani, Stewart Slocum, Usman Anwar, Anand Siththanjan, Max Nadeau, Eric J. Michaud, Jacob Pfau, Dmitrii Krasheninnikov, Xin Chen, Lauro Langosco, Peter Hase, Erdem Biyik, Anca D. Dragan, David Krueger, Dorsa Sadigh, and Dylan Hadfield-Menell. Open Problems and Fundamental Limitations of Reinforcement Learning from Human Feedback. *Transactions on Machine Learning Research (TMLR)*, 2023.

Ján Cegin, Jakub Simko, and Peter Brusilovsky. ChatGPT to Replace Crowdsourcing of Paraphrases for Intent Classification: Higher Diversity and Comparable Model Robustness. In *Proceedings of the 2023 Conference on Empirical Methods in Natural Language Processing (EMNLP)*, 2023.

Robert J. Fowler, Michael S. Paterson, and Steven L. Tanimoto. Optimal Packing and Covering in the Plane are NP-complete. *Information Processing Letters*, 12(3):133–137, 1981.

Aishwarya Kamath et al. Gemma 3 Technical Report. *CoRR*, abs/2503.19786, 2025.

Hannah Rose Kirk, Bertie Vidgen, Paul Röttger, and Scott A. Hale. Personalisation Within Bounds: A Risk Taxonomy and Policy Framework for the Alignment of Large Language Models with Personalised Feedback. *CoRR*, abs/2303.05453, 2023.

Grgur Kovac, Masataka Sawayama, Rémy Portelas, Cédric Colas, Peter Ford Dominey, and Pierre-Yves Oudeyer. Large Language Models as Superpositions of Cultural Perspectives. *CoRR*, abs/2307.07870, 2023.

Andreas Krause and Daniel Golovin. Submodular Function Maximization. In *Tractability: Practical Approaches to Hard Problems*, pp. 71–104. 2014.

Preethi Lahoti, Nicholas Blumm, Xiao Ma, Raghavendra Kotikalapudi, Sahitya Potluri, Qijun Tan, Hansa Srinivasan, Ben Packer, Ahmad Beirami, Alex Beutel, and Jilin Chen. Improving Diversity of Demographic Representation in Large Language Models via Collective-Critiques and Self-Voting. In *Proceedings of the 2023 Conference on Empirical Methods in Natural Language Processing (EMNLP)*, 2023.

Messi H. J. Lee, Jacob M. Montgomery, and Calvin K. Lai. Large Language Models Portray Socially Subordinate Groups as More Homogeneous, Consistent with a Bias Observed in Humans. In *ACM Conference on Fairness, Accountability, and Transparency (FAccT)*, 2024.

Ruibo Liu, Ge Zhang, Xinyu Feng, and Soroush Vosoughi. Aligning Generative Language Models with Human Values. In *Findings of the Association for Computational Linguistics: NAACL*, 2022.

Ryan Liu, Theodore R. Sumers, Ishita Dasgupta, and Thomas L. Griffiths. How do Large Language Models Navigate Conflicts between Honesty and Helpfulness? In *Forty-first International Conference on Machine Learning (ICML)*, 2024.

Julia M. Markel, Steven G. Opferman, James A. Landay, and Chris Piech. GPTeach: Interactive TA Training with GPT-based Students. In *Proceedings of the Tenth ACM Conference on Learning @ Scale (L@S)*, 2023.

Robert R. McCrae and Oliver P. John. An Introduction to the Five-factor Model and its Applications. *Journal of personality*, 60 2:175–215, 1992.

Leland McInnes and John Healy. UMAP: Uniform Manifold Approximation and Projection for Dimension Reduction. *CoRR*, abs/1802.03426, 2018.

Baharan Mirzasoleiman, Ashwinkumar Badanidiyuru, Amin Karbasi, Jan Vondrák, and Andreas Krause. Lazier Than Lazy Greedy. In *Proceedings of the Twenty-Ninth AAAI Conference on Artificial Intelligence (AAAI)*, 2015.

Youssef Mohamed, Faizan Farooq Khan, Kilichbek Haydarov, and Mohamed Elhoseiny. It is Okay to Not Be Okay: Overcoming Emotional Bias in Affective Image Captioning by Contrastive Data Collection. In *IEEE/CVF Conference on Computer Vision and Pattern Recognition (CVPR)*, 2022.

Saif M. Mohammad and Svetlana Kiritchenko. WikiArt Emotions: An Annotated Dataset of Emotions Evoked by Art. In *Proceedings of the Eleventh International Conference on Language Resources and Evaluation (LREC)*, 2018.

Daniil Moskovskiy, Sergey Pletnev, and Alexander Panchenko. LLMs to Replace Crowdsourcing For Parallel Data Creation? The Case of Text Detoxification. In *Findings of the Association for Computational Linguistics: EMNLP*, 2024.

George L. Nemhauser, Laurence A. Wolsey, and Marshall L. Fisher. An Analysis of Approximations for Maximizing Submodular Set Functions - I. *Math. Program.*, 14(1), 1978.

Manh Hung Nguyen, Sebastian Tschiatschek, and Adish Singla. Large Language Models for In-Context Student Modeling: Synthesizing Student’s Behavior in Visual Programming. In *Proceedings of the 17th International Conference on Educational Data Mining (EDM)*, 2024.

Long Ouyang, Jeffrey Wu, Xu Jiang, Diogo Almeida, Carroll L. Wainwright, Pamela Mishkin, Chong Zhang, Sandhini Agarwal, Katarina Slama, Alex Ray, John Schulman, Jacob Hilton, Fraser Kelton, Luke Miller, Maddie Simens, Amanda Askell, Peter Welinder, Paul F. Christiano, Jan Leike, and Ryan Lowe. Training Language Models to Follow Instructions with Human Feedback. In *Advances in Neural Information Processing Systems 35: Annual Conference on Neural Information Processing Systems (NeurIPS)*, 2022.

Aida Ramezani and Yang Xu. Knowledge of Cultural Moral Norms in Large Language Models. In *Proceedings of the 61st Annual Meeting of the Association for Computational Linguistics (ACL)*, 2023.

Beatrice Rammstedt and Oliver P. John. Measuring Personality in One Minute or Less: A 10-item Short Version of the Big Five Inventory in English and German. *Journal of Research in Personality*, 41(1):203–212, 2007.

Leonard Salewski, Stephan Alaniz, Isabel Rio-Torto, Eric Schulz, and Zeynep Akata. In-Context Impersonation Reveals Large Language Models’ Strengths and Biases. In *Advances in Neural Information Processing Systems 36: Annual Conference on Neural Information Processing Systems (NeurIPS)*, 2023.

Shibani Santurkar, Esin Durmus, Faisal Ladhak, Cinoo Lee, Percy Liang, and Tatsunori Hashimoto. Whose Opinions Do Language Models Reflect? In *International Conference on Machine Learning (ICML)*, 2023.

Adish Singla, Eric Horvitz, Ece Kamar, and Ryen White. Stochastic Privacy. In *Proceedings of the Twenty-Eighth AAAI Conference on Artificial Intelligence (AAAI)*, 2014.

Seungjong Sun, Eungu Lee, Dongyan Nan, Xiangying Zhao, Wonbyung Lee, Bernard J. Jansen, and Jang-Hyun Kim. Random Silicon Sampling: Simulating Human Sub-Population Opinion Using a Large Language Model Based on Group-Level Demographic Information. *CoRR*, abs/2402.18144, 2024.

Xiaofei Sun, Xiaoya Li, Jiwei Li, Fei Wu, Shangwei Guo, Tianwei Zhang, and Guoyin Wang. Text Classification via Large Language Models. In *Findings of the Association for Computational Linguistics: EMNLP*, 2023.

Wei Ren Tan, Chee Seng Chan, Hernan Aguirre, and Kiyoshi Tanaka. Improved ArtGAN for Conditional Synthesis of Natural Image and Artwork. *IEEE Transactions on Image Processing*, 28(1):394–409, 2019.

Yan Tao, Olga Viberg, Ryan S Baker, and René F Kizilcec. Cultural Bias and Cultural Alignment of Large Language Models. *PNAS Nexus*, 3(9):pgae346, 2024.

Vedat Verter. Uncapacitated and Capacitated Facility Location Problems. In *Foundations of Location Analysis*, pp. 25–37. New York, NY, 2011.

Zichao Wang, Angus Lamb, Evgeny Saveliev, Pashmina Cameron, Yordan Zaykov, José Miguel Hernández-Lobato, Richard E. Turner, Richard G. Baraniuk, Craig Barton, Simon Peyton Jones, Simon Woodhead, and Cheng Zhang. Diagnostic Questions: The NeurIPS 2020 Education Challenge. *CoRR*, abs/2007.12061, 2020.

Emily Wenger and Yoed N. Kenett. We’re Different, We’re the Same: Creative Homogeneity Across LLMs. *CoRR*, abs/2501.19361, 2025.

Chengxing Xie, Canyu Chen, Feiran Jia, Ziyu Ye, Shiyang Lai, Kai Shu, Jindong Gu, Adel Bibi, Ziniu Hu, David Jurgens, James Evans, Philip Torr, Bernard Ghanem, and Guohao Li. Can Large Language Model Agents Simulate Human Trust Behavior? In *Advances in Neural Information Processing Systems 38: Annual Conference on Neural Information Processing Systems (NeurIPS)*, 2024.

Se-eun Yoon, Zhankui He, Jessica Maria Echterhoff, and Julian J. McAuley. Evaluating Large Language Models as Generative User Simulators for Conversational Recommendation. In *Proceedings of the 2024 Conference of the North American Chapter of the Association for Computational Linguistics: Human Language Technologies (Volume 1: Long Papers)*, NAACL, 2024.

Ruoyu Zhang, Yanzeng Li, Yongliang Ma, Ming Zhou, and Lei Zou. LLMaAA: Making Large Language Models as Active Annotators. In *Findings of the Association for Computational Linguistics: EMNLP*, 2023.

Zheyuan Zhang, Daniel Zhang-Li, Jifan Yu, Linlu Gong, Jinchang Zhou, Zhanxin Hao, Jianxiao Jiang, Jie Cao, Huiqin Liu, Zhiyuan Liu, Lei Hou, and Juanzi Li. Simulating Classroom Education with LLM-Empowered Agents. In *Proceedings of the 2025 Conference of the Nations of the Americas Chapter of the Association for Computational Linguistics: Human Language Technologies (NAACL)*, 2025.

APPENDIX

A TABLE OF CONTENTS

In this section, we briefly describe the content provided in the paper’s appendices.

- Section [B](#) provides more details about the experimental setup, including datasets and prompts used for each domain, computational resources.
- Section [C](#) provides results on multiple runs with different context sizes K and random seeds.
- Section [D](#) provides detailed proofs of our theorems and propositions.

B ADDITIONAL EXPERIMENTAL SETUP

B.1 EEDI

Dataset. We use the EEDI math dataset (Wang et al., 2020), which provides data on students’ answers to mathematics questions on the Eedi platform. The questions are multiple-choice with four answer choices presented as images, and we select 40 that can be converted to text and have a large number of student responses, chosen to maximize both the number of questions answered per student and the number of students answering each question. The selected questions cover four concepts—Fractions, Negative Numbers, Mental Multiplication and Division, and Simplifying Expressions—with half of the questions in each concept used for training and the other half for testing.

Prompt for agent. Each agent is given a set of K demonstrations, which are pairs of math questions and example answers provided by the real students (cf. Figure 5). Then, we ask the agent to analyze the given answers and predict how the student would answer a new question.

Figure 5: [EEDI] Prompt for Agent with K demonstrations

```
[User message]  
{question_1}  
{example_answer_of_question_1}  
. . .  
{question_K}  
{example_answer_of_question_K}
```

Evaluate whether the student’s previous answers reveal any misconceptions. If so, analyze those misconceptions before proceeding. If not, directly predict how the student would answer the following question.

```
{question}
```

B.2 OPINIONQA

Dataset. We use questions and answers from the US citizens in the American Trends Panel W92 survey data, which was used in (Santurkar et al., 2023). This survey includes 77 multiple-choice questions related to politics and responses from over 10,000 respondents across the US. The answer choices typically have an ordinal structure (e.g., ranging from “A great deal” to “Not at all”) and we reuse the mapping from answer choices to ordinal values from (Santurkar et al., 2023). In addition, the survey data includes demographic information of the people, including ideology, political party and region. We sample $N = 500$ people and take their answers to create our dataset. We use the demographic information of these people for analysis purposes only.

Prompt for agent. Each agent is given a set of K demonstrations, which are pairs of questions and example answers provided by the real survey respondents (cf. Figure 6). Then, we ask the agent to act as the human who has given the answers above and to answer a new question.

Figure 6: [OpinionQA] Prompt for Agent with K demonstrations

```
[User message]  
{question_1}  
{example_answer_of_question_1}  
. . .  
{question_K}  
{example_answer_of_question_K}
```

Act as the human who has given the answers above. Answer the following question.
{question}

B.3 WIKIART

Figure 7: [Wikiart] Prompt for Synthetic Human

[System message] Act as a human who has taken the following personality test. Be mindful of how you focus your attention and the way you express yourself through language.
I see myself as someone who is generally trusting: {answer}
I see myself as someone who tends to be lazy: {answer}
I see myself as someone who is relaxed, handles stress well: {answer}
I see myself as someone who has few artistic interests: {answer}
I see myself as someone who is outgoing, sociable: {answer}
I see myself as someone who tends to find fault with others: {answer}
I see myself as someone who does a thorough job: {answer}
I see myself as someone who gets nervous easily: {answer}
I see myself as someone who has an active imagination: {answer}
[User message] What emotions does the following painting evoke? Choose from the following list of emotions: gratitude, happiness, humility, love, optimism, trust, anger, arrogance, disgust, fear, pessimism, regret, sadness, shame, agreeableness, anticipation, disagreeableness, shyness, surprise. Provide a short explanation referencing specific details from the painting. Respond in JSON format with two keys: "emotions" and "explanation".
{painting}

Figure 8: [Wikiart] Prompt for extracting embeddings for an annotator

[User message]
Response_1: annotation_of_painting_1
. . .
Response_q: annotation_of_painting_q

Figure 9: [Wikiart] Prompt for Agent with K demonstrations

[User message]
{painting_1}
{annotation_of_painting_1}
. . .
{painting_K}
{annotation_of_painting_K}
Act as the human who has given the answers above. What emotions does the following painting evoke? Choose from the following list of emotions: gratitude, happiness, humility, love, optimism, trust, anger, arrogance, disgust, fear, pessimism, regret, sadness, shame, agreeableness, anticipation, disagreeableness, shyness, surprise. Provide a short explanation referencing specific details from the painting. Respond in JSON format with two keys: "emotions" and "explanation".
{painting}

Dataset. We use LLMs conditioned on the Big Five personality traits (McCrae & John, 1992), namely Extraversion, Agreeableness, Conscientiousness, Emotional Stability, and Openness, to act as annotators. Each annotator is specified by responses to a 10-item BFI questionnaire (Rammstedt & John, 2007), which we place in the system message to instruct the LLM to act as a human who has taken the test (cf. Figure 7). Responses take one of five values (Disagree Strongly, Disagree a Little, Neither Agree nor Disagree, Agree a Little, Agree Strongly), which we convert into trait scores using the formula in (Rammstedt & John, 2007) and rescale to [0, 5], where higher values

indicate stronger expression of the trait. To create a diverse set of annotators, we sample responses from normal distributions of trait values with varying means and standard deviations. These system messages condition the LLM to act with distinct personalities, and we use Gemma3-27B (Kamath et al., 2025) to generate their answers.

To create an embedding for each human or agent, we concatenate their answers on the train/test tasks into a single prompt (cf. Figure 8), pass it through a language model (Gemma3-12B (Kamath et al., 2025)), and extract the last hidden state with mean pooling to obtain the embedding. We then reduce the dimensionality to 64 using PCA and measure distances between embeddings using L2 distance.

Prompt for agent. Each agent is given a set of K demonstrations, which are pairs of paintings and example annotations provided by the annotators (cf. Figure 9). Then, we ask the agent to act as the annotator who has given the answers above and to annotate a new painting. The LLM agent is given a list of emotions (from (Mohammad & Kiritchenko, 2018)) to choose from, and it must provide a short explanation referencing specific details from the painting.

B.4 RESOURCES

We use a machine with 2 x Intel Xeon Gold 5317 for all experiments. We use 1 x NVIDIA H100 80GB for experiments on EEDI and OpinionQA datasets, and 1 x NVIDIA H200 141GB for Wikiart dataset.

C ADDITIONAL EXPERIMENTAL RESULTS

In this section, we show results on different context sizes $K = 1, 3, 5$ for each dataset. We report the mean and standard error (shown as error bars) computed over three seeds. Overall, we observe similar trends where our methods outperform other baselines across all datasets.

C.1 EEDI

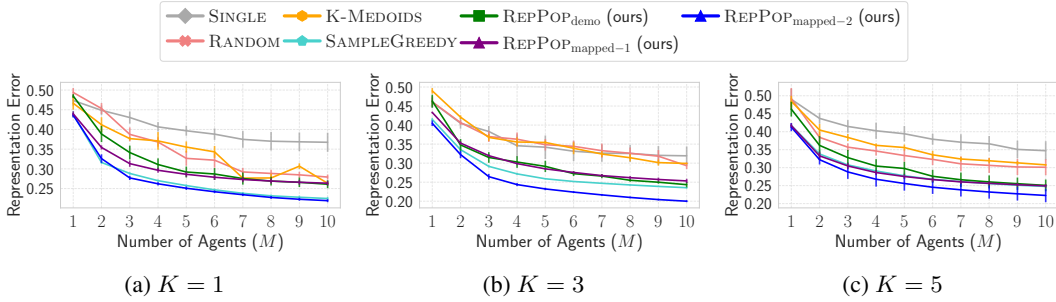


Figure 10: Representation error on EEDI dataset (Train).

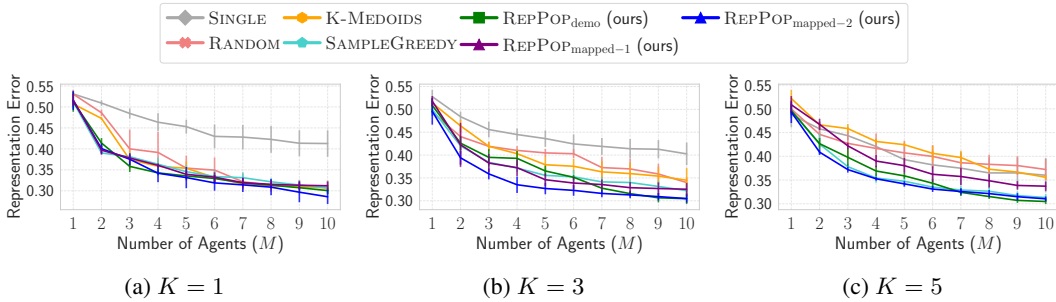


Figure 11: Representation error on EEDI dataset (Test).

C.2 OPINIONQA

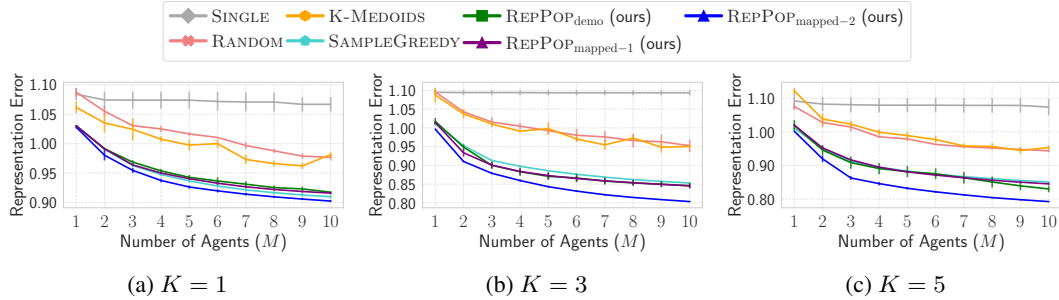


Figure 12: Representation error on OpinionQA dataset (Train).

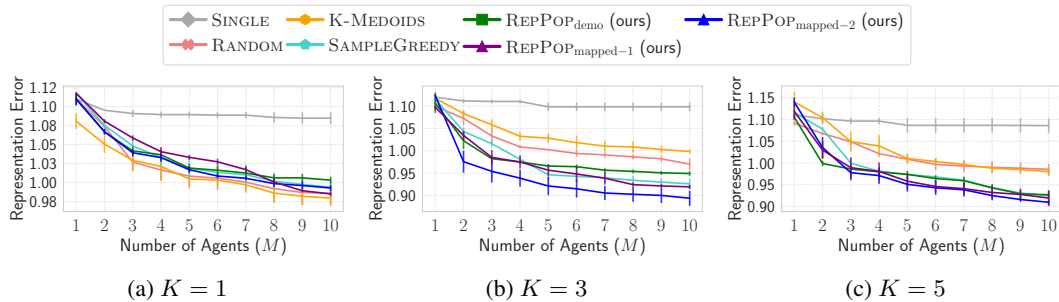


Figure 13: Representation error on OpinionQA dataset (Test).

C.3 WIKIART

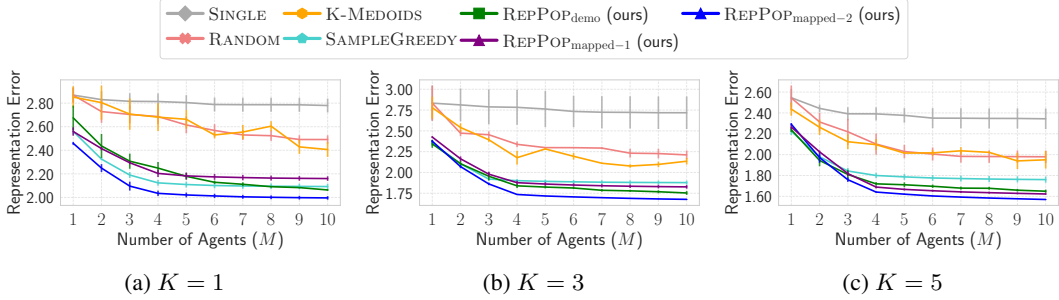


Figure 14: Representation error on Wikiart dataset (Train).

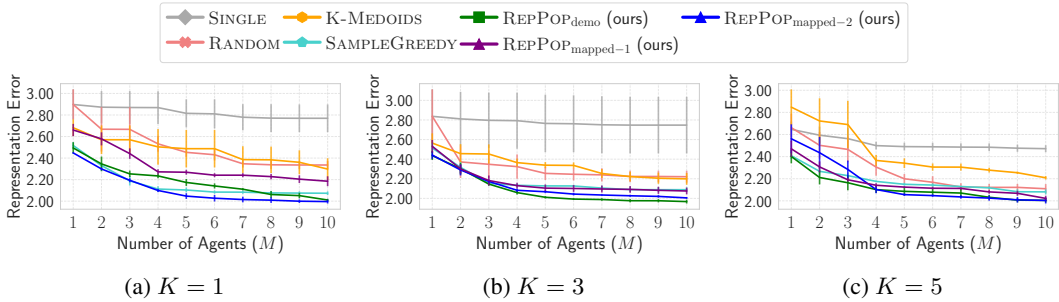


Figure 15: Representation error on Wikiart dataset (Test).

Agent behavior analysis. We select three agents and visualize the annotators they represent along with their aggregated traits (cf. Figure 16). For example, Agent 2 represents annotators with high neuroticism and low conscientiousness. To validate whether the agents exhibit behaviors consistent with the annotators they represent, we ask each constructed agent to complete the 10-item BFI test (Rammstedt & John, 2007), and their responses reveal traits that align with the average traits of the corresponding humans. For instance, Agent 2 in Figure 16 obtains the following trait scores: Extraversion (1.0), Agreeableness (1.5), Conscientiousness (1.38), Neuroticism (4.66), and Openness (2.5).

Embedding model analysis. We further evaluate our approach on the Wikiart dataset using a smaller and more efficient bidirectional encoder (gte-base-en-v1.5). The results in Table 5 confirm that our methods remain effective even when relying on a much smaller embedding model.

Table 5: Comparison of methods on the Wikiart dataset using the gte-base-en-v1.5 embedding model. We report the representation error on the test set with context size $K = 3$ and agent set size $M = 10$.

| Method | gte-base-en-v1.5 (137M) |
|-----------------------------------|-------------------------|
| SINGLE | 0.71 |
| RANDOM | 0.69 |
| K-MEDOIDS | 0.68 |
| SAMPLEGREEDY | 0.68 |
| REPPOP _{demo} (ours) | 0.62 |
| REPPOP _{mapped-1} (ours) | 0.66 |
| REPPOP _{mapped-2} (ours) | 0.68 |

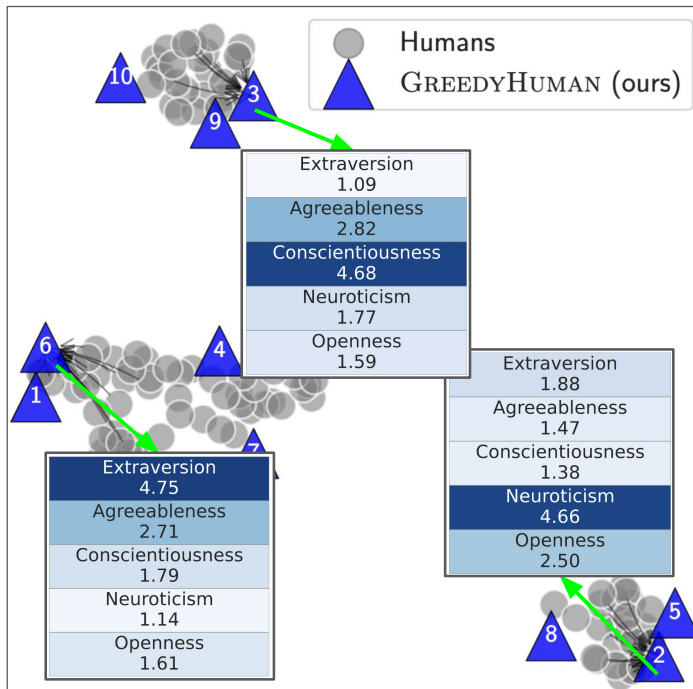


Figure 16: 2D embeddings of humans and agents constructed by REPPOP_{mapped-2} on $\mathcal{T}_{\text{train}}$ tasks in Wikiart dataset using UMAP (McInnes & Healy, 2018). We provide examples of aggregated traits (heatmaps) of annotators represented by each agent (connections are denoted by black arrows). We note that metadata are not used for constructing agents and used only for analysis. Our method REPPOP_{mapped-2} constructs agents to cover different areas in the annotator embedding space, collectively representing the annotators. Each agent represents a group of annotators with particular personality traits.

D PROOFS

D.1 PROOF OF THEOREM 1

Theorem 1 (NP-Hardness). The problem of selecting an optimal subset $L^* \subseteq \mathcal{L}$ of size M that maximizes $f(L)$ is NP-hard.

Proof. We show NP-hardness through a reduction from the k-facility location problem which extends the uncapacitated facility location problem (UFLP) by including a constraint on the maximum number of facilities. The problem is known to be NP-hard. (Fowler et al., 1981)

Consider an instance of the k-facility location problem with a set of potential facility locations $\mathcal{F} = \{f_1, f_2, \dots, f_{n_F}\}$, a set of customers $\mathcal{C} = \{c_1, c_2, \dots, c_{n_C}\}$, service costs $d(f, c)$ representing the cost of serving customer c from facility f , and a cardinality constraint M . The objective is to select a subset $F \subseteq \mathcal{F}$ of M facilities to minimize the sum of service costs $\sum_{c \in \mathcal{C}} \min_{f \in F} d(f, c)$.

We construct a corresponding instance of our representative agent selection problem as follows: set $\mathcal{H} = \mathcal{C}$ (each customer corresponds to a human); set $\mathcal{L} = \mathcal{F}$ (each potential facility location corresponds to a potential agent); define $\text{dist}(\mathbf{e}_h, \mathbf{e}_l) = d(l, h)$ for each human $h \in \mathcal{H}$ and agent $l \in \mathcal{L}$; and set M to be the number of facilities we wish to open.

Under this construction, our objective function becomes:

$$\begin{aligned} f(L) &= \frac{1}{|\mathcal{H}|} \sum_{h \in \mathcal{H}} \left[D_{\max} - \min_{l \in L} d(l, h) \right] \\ &= \frac{1}{|\mathcal{H}|} \left(\sum_{h \in \mathcal{H}} D_{\max} \right) - \frac{1}{|\mathcal{H}|} \sum_{h \in \mathcal{H}} \min_{l \in L} d(l, h) \\ &= D_{\max} - \frac{1}{|\mathcal{H}|} \sum_{h \in \mathcal{H}} \min_{l \in L} d(l, h) \end{aligned}$$

Since D_{\max} is a constant and $\frac{1}{|\mathcal{H}|}$ is a positive constant, maximizing $f(L)$ is equivalent to minimizing $\sum_{h \in \mathcal{H}} \min_{l \in L} d(l, h)$, which is the objective of the k-facility location problem.

Therefore, if the representative agent selection problem could be solved in polynomial time, the k-facility location problem could also be solved in polynomial time. Since the k-facility location problem is NP-hard, the representative agent selection problem must also be NP-hard. \square

D.2 PROOF OF PROPOSITION 1

Proposition 1 (Submodularity). The objective function

$$f(L) = \frac{1}{|\mathcal{H}|} \sum_{h \in \mathcal{H}} \left[D_{\max} - \min_{l \in L} \text{dist}(\mathbf{e}_h, \mathbf{e}_l) \right]$$

is submodular.

Proof. A set function f is submodular if for all $A \subseteq B \subseteq \mathcal{L}$ and for all $l' \in \mathcal{L} \setminus B$, we have $f(A \cup \{l'\}) - f(A) \geq f(B \cup \{l'\}) - f(B)$.

Let $A \subseteq B \subseteq \mathcal{L}$ and $l' \in \mathcal{L} \setminus B$. The marginal gain of adding l' to A is:

$$f(A \cup \{l'\}) - f(A) = \frac{1}{|\mathcal{H}|} \sum_{h \in \mathcal{H}} \left[D_{\max} - \min_{l \in A \cup \{l'\}} \text{dist}(\mathbf{e}_h, \mathbf{e}_l) - \left(D_{\max} - \min_{l \in A} \text{dist}(\mathbf{e}_h, \mathbf{e}_l) \right) \right]$$

This simplifies to:

$$f(A \cup \{l'\}) - f(A) = \frac{1}{|\mathcal{H}|} \sum_{h \in \mathcal{H}} \left[\min_{l \in A} \text{dist}(\mathbf{e}_h, \mathbf{e}_l) - \min_{l \in A \cup \{l'\}} \text{dist}(\mathbf{e}_h, \mathbf{e}_l) \right]$$

Define $\mathcal{H}_A^{l'} = \{h \in \mathcal{H} \mid \text{dist}(\mathbf{e}_h, \mathbf{e}_{l'}) < \min_{l \in A} \text{dist}(\mathbf{e}_h, \mathbf{e}_l)\}$ as the set of humans for whom l' provides improvement when added to A . Similarly define $\mathcal{H}_B^{l'}$ for set B .

For humans in $h \in \mathcal{H} \setminus \mathcal{H}_A^{l'}$, the closest agent in A remains closer than l' , so $\min_{l \in A \cup \{l'\}} \text{dist}(\mathbf{e}_h, \mathbf{e}_l) = \min_{l \in A} \text{dist}(\mathbf{e}_h, \mathbf{e}_l)$, giving zero marginal improvement. Therefore:

$$f(A \cup \{l'\}) - f(A) = \frac{1}{|\mathcal{H}|} \sum_{h \in \mathcal{H}_A^{l'}} \left[\min_{l \in A} \text{dist}(\mathbf{e}_h, \mathbf{e}_l) - \text{dist}(\mathbf{e}_h, \mathbf{e}_{l'}) \right]$$

Since $A \subseteq B$, for any human h , we have $\min_{l \in A} \text{dist}(\mathbf{e}_h, \mathbf{e}_l) \geq \min_{l \in B} \text{dist}(\mathbf{e}_h, \mathbf{e}_l)$.

This implies that if l' provides improvement over B (i.e., $h \in \mathcal{H}_B^{l'}$), then l' also provides improvement over A (i.e., $h \in \mathcal{H}_A^{l'}$). Therefore, $\mathcal{H}_B^{l'} \subseteq \mathcal{H}_A^{l'}$.

For humans in $\mathcal{H}_B^{l'}$, the improvement when adding l' to A is at least as large as when adding l' to B , since $\min_{l \in A} \text{dist}(\mathbf{e}_h, \mathbf{e}_l) - \text{dist}(\mathbf{e}_h, \mathbf{e}_{l'}) \geq \min_{l \in B} \text{dist}(\mathbf{e}_h, \mathbf{e}_l) - \text{dist}(\mathbf{e}_h, \mathbf{e}_{l'})$.

Similarly, for B we have:

$$f(B \cup \{l'\}) - f(B) = \frac{1}{|\mathcal{H}|} \sum_{h \in \mathcal{H}_B^{l'}} \left[\min_{l \in B} \text{dist}(\mathbf{e}_h, \mathbf{e}_l) - \text{dist}(\mathbf{e}_h, \mathbf{e}_{l'}) \right]$$

Therefore:

$$\begin{aligned} f(A \cup \{l'\}) - f(A) &= \frac{1}{|\mathcal{H}|} \sum_{h \in \mathcal{H}_A^{l'}} \left[\min_{l \in A} \text{dist}(\mathbf{e}_h, \mathbf{e}_l) - \text{dist}(\mathbf{e}_h, \mathbf{e}_{l'}) \right] \\ &= \frac{1}{|\mathcal{H}|} \sum_{h \in \mathcal{H}_B^{l'}} \left[\min_{l \in A} \text{dist}(\mathbf{e}_h, \mathbf{e}_l) - \text{dist}(\mathbf{e}_h, \mathbf{e}_{l'}) \right] \\ &\quad + \frac{1}{|\mathcal{H}|} \sum_{h \in \mathcal{H}_A^{l'} \setminus \mathcal{H}_B^{l'}} \left[\min_{l \in A} \text{dist}(\mathbf{e}_h, \mathbf{e}_l) - \text{dist}(\mathbf{e}_h, \mathbf{e}_{l'}) \right] \\ &\geq \frac{1}{|\mathcal{H}|} \sum_{h \in \mathcal{H}_B^{l'}} \left[\min_{l \in B} \text{dist}(\mathbf{e}_h, \mathbf{e}_l) - \text{dist}(\mathbf{e}_h, \mathbf{e}_{l'}) \right] \\ &= f(B \cup \{l'\}) - f(B) \end{aligned}$$

This shows that f is submodular. □

D.3 PROOF OF THEOREM 2

Theorem 2 (Performance Guarantee for REPPOP_{mapped-1} and REPPOP_{mapped-2}). Let $\tilde{\mathcal{L}} = \{l_h \mid h \in \mathcal{H}\}$ be the proxy agent set where for each $h \in \mathcal{H}$, $l_h \in N_\rho(h)$, with $N_\rho(h)$ representing the ρ -neighborhood of h . Define the human coverage ratio $\gamma = \frac{f(L_{\mathcal{H}}^*)}{f(L_{\tilde{\mathcal{L}}}^*)} \in [0, 1]$, where $L_{\mathcal{H}}^*$ is the optimal subset from the human set and $L_{\tilde{\mathcal{L}}}^*$ is the optimal subset from the full agent set. If $L_{\tilde{\mathcal{L}}}^{\text{greedy}}$ is the subset of size M returned by the greedy algorithm on $\tilde{\mathcal{L}}$, then:

$$f(L_{\tilde{\mathcal{L}}}^{\text{greedy}}) \geq (1 - \frac{1}{e})(\gamma \cdot f(L_{\mathcal{L}}^*) - \rho)$$

Proof. In our context, $L_{\mathcal{H}}^* \subseteq \mathcal{H}$ represents the optimal subset of humans of size M that would be selected if we directly choose humans instead of agents. This is a theoretical construct for analysis purposes. In contrast, $L_{\mathcal{L}}^*$ is the optimal subset of size M from the actual agent set \mathcal{L} . The human coverage ratio $\gamma = \frac{f(L_{\mathcal{H}}^*)}{f(L_{\mathcal{L}}^*)} \in [0, 1]$ measures how well selecting from the human set can approximate

the optimal solution achievable using the full agent set. We start our proof by first decomposing the objective function as

$$f(L) = \sum_{h \in \mathcal{H}} f_h(L)$$

where

$$f_h(L) = \frac{1}{|\mathcal{H}|} \left[D_{\max} - \min_{l \in L} \text{dist}(\mathbf{e}_h, \mathbf{e}_l) \right]$$

For each human h in the optimal subset $L_{\mathcal{H}}^*$, consider its corresponding agent l_h in the proxy agent set $\tilde{\mathcal{L}}$. Let $L_{\tilde{\mathcal{L}}}^* = \{l_h | h \in L_{\mathcal{H}}^*\}$.

By definition, for each human $h \in \mathcal{H}$ and its corresponding proxy agent $l_h \in \tilde{\mathcal{L}}$, we have $\text{dist}(\mathbf{e}_h, \mathbf{e}_{l_h}) \leq \rho$ since l_h is in the ρ -neighborhood of h . Therefore:

$$|f_h(L_{\mathcal{H}}^*) - f_h(L_{\tilde{\mathcal{L}}}^*)| \leq \frac{\rho}{|\mathcal{H}|}$$

The above inequality holds because the maximum distance deviation between any human and its proxy agent is at most ρ (by definition of the ρ -neighborhood).

Then:

$$|f(L_{\mathcal{H}}^*) - f(L_{\tilde{\mathcal{L}}}^*)| = \left| \sum_{h \in \mathcal{H}} f_h(L_{\mathcal{H}}^*) - f_h(L_{\tilde{\mathcal{L}}}^*) \right| \leq \sum_{h \in \mathcal{H}} |f_h(L_{\mathcal{H}}^*) - f_h(L_{\tilde{\mathcal{L}}}^*)| \leq \frac{\rho}{|\mathcal{H}|} \cdot |\mathcal{H}| = \rho$$

This gives us:

$$f(L_{\tilde{\mathcal{L}}}^*) \geq f(L_{\mathcal{H}}^*) - \rho \quad (2)$$

Since $L_{\tilde{\mathcal{L}}}^*$ is the optimal subset of size M from the proxy agent set $\tilde{\mathcal{L}}$, and $L_{\tilde{\mathcal{L}}}^*$ is a feasible solution of size M from $\tilde{\mathcal{L}}$, we have:

$$f(L_{\tilde{\mathcal{L}}}^*) \geq f(L_{\tilde{\mathcal{L}}}^*) \quad (3)$$

From the guarantees of the greedy algorithm for submodular function maximization (Nemhauser et al., 1978), if $L_{\tilde{\mathcal{L}}}^{greedy}$ is the subset of size M returned by the greedy algorithm on $\tilde{\mathcal{L}}$, we have:

$$f(L_{\tilde{\mathcal{L}}}^{greedy}) \geq (1 - \frac{1}{e})f(L_{\tilde{\mathcal{L}}}^*) \quad (4)$$

Combining inequalities equation 2, equation 3, and equation 4, we get:

$$f(L_{\tilde{\mathcal{L}}}^{greedy}) \geq (1 - \frac{1}{e})f(L_{\tilde{\mathcal{L}}}^*) \geq (1 - \frac{1}{e})f(L_{\tilde{\mathcal{L}}}^*) \geq (1 - \frac{1}{e})(f(L_{\mathcal{H}}^*) - \rho)$$

Using the definition of human coverage ratio $\gamma = \frac{f(L_{\mathcal{H}}^*)}{f(L_{\tilde{\mathcal{L}}}^*)}$, we have $f(L_{\mathcal{H}}^*) = \gamma \cdot f(L_{\tilde{\mathcal{L}}}^*)$. Substitution yields

$$f(L_{\tilde{\mathcal{L}}}^{greedy}) \geq (1 - \frac{1}{e})(\gamma \cdot f(L_{\tilde{\mathcal{L}}}^*) - \rho)$$

This gives us the performance guarantees for REPOP_{mapped-1} and REPOP_{mapped-2}. \square